Design of EFGR kinase domain inhibitors for the potential treatment of lung and other cancers

Jodie Meng
Advisor: John Thurmond
Illinois Mathematics and Science Academy

INTRODUCTION

In 2018 alone, over 18 million cancer-related cases were diagnosed and 9.5 million cancer-related deaths occurred worldwide. As a small-molecule drug orally administered for the treatment of lung and pancreatic cancer, erlotinib (Tarceva®) inhibits the phosphorylation of the tyrosine kinase domain in the Epidermal Growth Factor Receptor (EGFR). Inhibition of EGFR reduces the bioactivity of tumor-associated endothelial cells and interferes with signal pathways involved in metastasis and development of angiogenesis. Increase in drug concentration leads to adverse effects, ranging from rash and nausea to gastrointestinal bleeding, perforation, hepatic failure, among others. Therefore, it is desirable to reduce the toxicity and increase potency of the drug to increase its clinical applicability. This study focuses on using structure-based drug design techniques in the early drug discovery process. Computer programs like SeeSar, AdmetSar, SwissAdme, and LabMol allow for the prediction of pharmacokinetic and pharmacodynamic parameters. The goal of the study was to design more advantageous compounds to erlotinib, gefitinib, and a second-generation TKI (compound 1), and provide evidence supporting a computer-aided approach to drug discovery.

METHODOLOGY

SeeSar Modification

The crystal structure of the Epidermal Growth Factor Receptor tyrosine kinase domain in complex with the 4-anilinoquinazoline inhibitor of erlotinib was obtained from the Protein Data Bank (Code: 1M17). Components of erlotinib, including the 1,2-dimethoxyethane, quinazoline, and imidogen structures were isolated and modified through the replacement of bioisosteres, addition of aromatic rings, addition of OH groups, and the strengthening of structural rigidity. Candidate drugs predicted to inhibit EGFR with a strong binding affinity, as determined by the estimated ligand-lipophilicity efficiency (LLE), torsion, and Inter/Intra clash were designed. Using Lipinski's rule of five (<5 hydrogen bond donors, <5 hydrogen bond acceptors, <500 g/mol, <5 logP), drugs with promising physicochemical characteristics for oral activity in humans were selected.

Property Prediction

AdmetSar allowed for the prediction of the compound's ADMET (absorption, distribution, metabolism, excretion, and toxicity) properties. Predictive models were based upon a collection of about 96 thousand compounds. SwissAdme also offered comprehensive prediction services and the generation of models including BOILED-egg and the Bioavailability Radar. LabMol allowed for the prediction of the molecule's cardiotoxic effects via hERG inhibition.

RESULTS

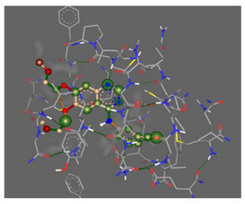

The figure above represents the erlotinib's interactions with the protein. The colored coronas indicate the contribution of each atom to the molecule's binding affinity. Green indicates a positive contribution, while red indicates a negative contribution. White blurs depict unoccupied space within the binding site. The color of the bonds indicates the contribution to the molecule's torsion. The average estimated binding affinity is 5092 nM.

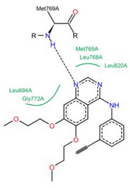

The figure above s a 2-dimensional diagram of erlotinib's interactions with surrounding amino acids. Dotted lines indicate hydrogen bonds between the ligand the protein, salt bridges, and/or metal interactions. Green contour lines represent hydrophobic interactions.

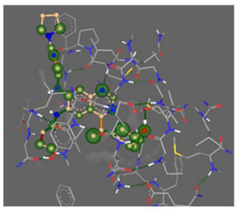

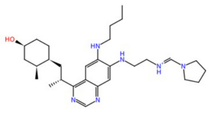

The figures above depict designed compound 2. It has notable modifications including extensions of the substituents on quinazoline. It has an average estimated binding affinity of 0.00269 nM.

Erlotinib data Retrieved from AdmetSar

Side Effect	Value	Probability
Carcinogenicity (binary)	-	0.9286
Carcinogenicity (trinary)	Non-required	0.5393
Eye corrosion	-	0.9897
Eye irritation	-	0.9683
Ames mutagenesis	-	0.57
Human either-a-go-go inhibition	+	0.6978
micronuclear	+	0.79
Hepatotoxicity	+	0.725
Acute Oral Toxicity (c)	III	0.6971
Estrogen receptor binding	+	0.8023
Androgen receptor binding	+	0.8696
Thyroid receptor binding	+	0.836
Glucocorticoid receptor binding	+	0.8971
Aromatase binding	+	0.8686
PPAR gamma	+	0.7436

Compound 2 Data Retrieved from AdmetSar

Side Effect	Value	Probability
Carcinogenicity (binary)	-	0.7714
Carcinogenicity (trinary)	Non-required	0.6508
Eye corrosion	-	0.9844
Eye irritation	-	0.9794
Ames mutagenesis	-	0.67
Human either-a-go-go inhibition	+	0.7917
micronuclear	+	0.76
Hepatotoxicity	-	0.5
Acute Oral Toxicity (c)	III	0.6025
Estrogen receptor binding	+	0.6001
Androgen receptor binding	+	0.6923
Thyroid receptor binding	+	0.5514
Glucocorticoid receptor binding	-	0.4772
Aromatase binding	+	0.6793
PPAR gamma	-	0.5306

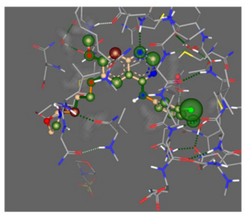

The figure above depicts the protein's interactions with gefitinib. The average estimated binding affinity is 170.35 nM.

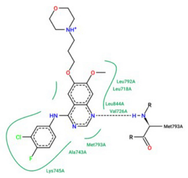

The figure above is a 2-dimensional diagram of the gefitinib interactions with surrounding amino acids. These include leucine, valine, methionine, valine, alanine, and lysine.

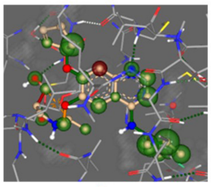

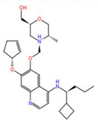

The figures above represent designed compound 3 with the highest improvement in binding affinity derived from gefitinib. It has an average estimated binding affinity of 0.00380 nM. Notable modifications include the replacement of a benzene ring with a cyclobutane, and the replacement of a nitrogen atom in the quinazoline with carbon.

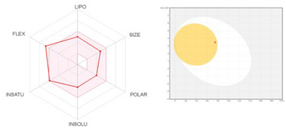

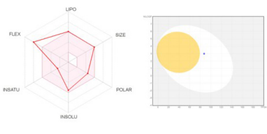

The graphics above depict the bioavailbility radar and BOILED-egg model for erlotinib (left) and compound 2 (right) as provided by SwissAdme. The bioavailability radar estimates six physicochemical properties: lipophilicity, size, polarity, solubility, flexibility and saturation. The pink region indicates the optimal range for each property. These parameters denote a XLOGP3 between -0.7 and + 5.0, MW between 150 and 500 g/mol, TPSA between 20 and 130 Å, logS less than or equal to 6, fraction of carbons in the sp 3 hybridization greater than or equal to 0.25, rotatable bonds less than or equal to 9. The BOILED-egg (Brain Or Intestinal. EstimateD permeation) model predicts a small molecule's gastrointestinal absorption or brain access based on lipophilicity and polarity. The white region indicates high probability of passive absorption into the gastrointestinal tract, while the yellow region indicates high probability of penetration into the blood-brain barrier. Furthermore, molecules are colored blue if they are predicted as actively effluxed by P-gp, or red if not a substrate of P-gp.

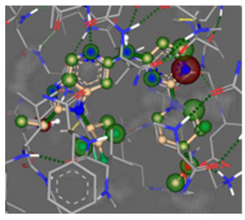

The figure above depicts the protein's interactions with the second-generation EGFR TKI, compound 1. The average estimated binding affinity is 805.47 nM.

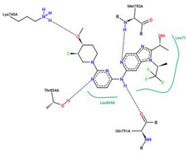

The figure above is a 2-dimensional diagram of the interactions between compound 1 and the surrounding amino acids.

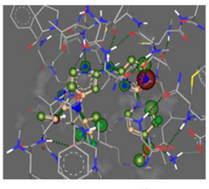

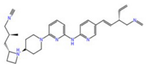

The figures above represent designed compound 4 with the highest improvement in binding affinity derived from compound 1 with a value of 0.0883 nM. Notable modifications include the extension of both carbon tails and the replacement of a nitrogen atom in the core fragment with a carbon atom.

Human Intestinal Absorption	+	0.9867
Caco-2	+	0.5686
Blood Brain Barrier	+	0.9778
Oral bioavailability	+	0.8143
Subcellular localization	Mitochondria	0.4954

Druglikeness	
Lipinski	Yes; 0 violation
Ghose	Yes
Veber	Yes
Egan	Yes
Muegge	Yes
Bioavailability Score	0.55
Medicinal Chemistry	
PAINS	0 alert
Brenk	1 alert: triple_bond
Leadlikeness	No; 2 violations: MW>350, Rotors>7
Synthetic accessibility	3.19

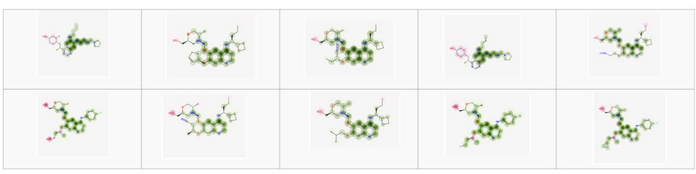

The figure above displays the top 10 designed compounds' (by binding affinity with 0 violations of Lipinski's rules) predicted ability to inhibit the Human Ether-a-go-go-related Gene (hERG) through probability maps of each fragment's contribution to hERG blockage. Lipinski's Rule of Five outlines molecular parameters important for a chemical's drug-likeness and potential for oral activity in humans. hERG potassium channels contribute to the electrical activity of the heart. Blockade of the channel may lead to cardiac arrhythmia.

Human Intestinal Absorption	+	0.8174
Caco-2	-	0.7197
Blood Brain Barrier	+	0.9801
Oral bioavailability	+	0.5429
Subcellular localization	Nucleus	0.4001

Druglikeness	
Lipinski	Yes; 0 violation
Ghose	No; 3 violations: MW>480, MR>130, #atoms>70
Veber	No; 1 violation: Rotors>10
Egan	Yes
Muegge	No; 1 violation: XLOGP3>5
Bioavailability Score	0.55
Medicinal Chemistry	
PAINS	0 alert
Brenk	2 alerts: imine_1, imine_2
Leadlikeness	No; 3 violations: MW>350, Rotors>7, XLOGP3>3.5
Synthetic accessibility	5.41

The tables above display information about the absorption and distribution of erlotinib (top) and compound 2 (bottom) upon entrance in the human body. The tables include a drug likeness section, which demonstrates each molecule's adherence to widely used drug rules, and a medicinal chemistry section, which offers information about PAINS and the molecule's ability to be synthesized in a lab.

CONCLUSION

Over 1400 unique molecules were designed and binding affinities were calculated by SeeSar. To increase binding affinity, 1,2-dimethoxyethane moiety was modified with nitrogen and additional aromatic rings and aromatic rings were added to imdogen linkers. Depending on molecular structure, the imdogen moiety was also altered. In order to decrease hERG binding, alcohol functional groups were added, more rigid bonds were constructed, and lipophilicity was decreased.

The best newly designed molecule, compound 2 had more interactions with amino acids and less unoccupied space. The estimated binding affinity was increased by over 1,800,000 fold, the compound had acceptable measures for bioactivity, however, was less synthetically accessible. The compound had improved toxicity but was more likely to inhibit hERG and other designed molecules were less likely to inhibit hERG. For future research we will be synthesizing the compound by modifying the synthetic pathway created by Yin et. al., for testing.

REFERENCES

Barreiro, E. (2005, February 25). Bioisosterism: a useful strategy for molecular modification and drug design. Retrieved January 7, 2019, from https://www.researchgate.net/publication/8092069_Bioisosterism_A_Useful_Strategy_for_Molecular_Modification_and_Drug_Design
Benet, L., Hosey, C., Ursu, O., & Oprea, T. (2016, June 1). BDDCS, the rule of 5 and drugability. Retrieved January 7, 2019, from https://www.ncbi.nlm.nih.gov/pmc/articles/PMC4910824/
Braga, R., Alves, V., & Silva, M. (2017). Pred-hERG: A novel web-accessible computational tool for predicting cardiac toxicity. Retrieved April 14, 2019, from https://www.ncbi.nlm.nih.gov/pmc/articles/PMC5720373/
Cancer. (2018, September 12). Retrieved January 10, 2019, from https://www.who.int/news-room/fact-sheets/detail/cancer
Cheng, F., Zhou, Y., Li, W., & Jie, S. (2012). admetSAR: a comprehensive source and free tool for assessment of chemical ADMET properties. Retrieved April 14, 2019, from https://www.ncbi.nlm.nih.gov/pubmed/23092397
Clay, D., Lipman, Y., & Bonk, M. E. (2005). *Erlotinib (Tarceva®): A brief overview*. Retrieved January 12, 2019, from https://www.ptcommunity.com/system/files/pdf/pj3010561_0.pdf
Daina, A., Michielin, O., & Zoete, V. (2017). SwissADME: a free web tool to evaluate pharmacokinetics, drug-likeness and medicinal chemistry friendliness of small molecules. Retrieved April 14, 2019, from https://www.nature.com/articles/srep42717
Del Rio, A., & Varchi, G. (2016). Molecular design of compounds targeting histone methyltransferases. In *Epi-Informatics*. Retrieved from https://www.sciencedirect.com/science/article/pii/B9780128028087000095
Dowell, J., Minna, J., & Kirkpatrick, P. (2005). Erlotinib hydrochloride. Retrieved April 14, 2019, from https://www.nature.com/articles/nrd1612
Erlotinib. (2013). Retrieved January 10, 2019, from https://toxnet.nlm.nih.gov/cgi-bin/sis/search/a?dbs+hsdb:@term+@DOCNO+8082
Julian, M. (2004). Current and emerging opportunities for molecular simulations in structure-based drug design. Retrieved April 14, 2019, from https://pubs.rsc.org/en/content/articlelanding/2014/cp/c3cp54164a#!divAbstract
Kelly, R., & Ko, A. (2008, March). Erlotinib in the treatment of advanced pancreatic cancer. Retrieved January 10, 2019, from https://www.ncbi.nlm.nih.gov/pmc/articles/PMC2727779/
Sasaki, T., Hiroki, K., & Yamashita, Y. (2013). The role of epidermal growth factor receptor in cancer metastasis and microenvironment. Retrieved January 7, 2019, from https://www.ncbi.nlm.nih.gov/pmc/articles/PMC3748428/
Wang, Y. (2012). Erlotinib in the treatment of advanced non-small cell lung cancer: An update for clinicians. Retrieved January 7, 2019, from https://www.ncbi.nlm.nih.gov/pmc/articles/PMC3244301/
Yin, X. J., Xu, G. H., Sun, X., Peng, Y., Ji, X., Jiang, K., & Li, F. (2010, June 11). Synthesis of bosutinib from 3-methoxy-4-hydroxybenzoic acid. Retrieved from https://www.ncbi.nlm.nih.gov/pubmed/20657439.